Lecture 7: Types of inverse problems, model reduction, model identication. Part B: Modal reduction for thermal problems: Core principles and presentation of the AROMM method

Frédéric Joly, Yassine Rouizi, Benjamin Gaume, Olivier Quéméner

Lecture 7: Types of inverse problems, model reduction, model identification.

Part B: Modal reduction for thermal problems: Core principles and presentation of the AROMM method

F. Joly, **Y. Rouizi**, **B. Gaume**, **O. Quéméner**

Laboratoire de Mécanique et d'Energétique d'Evry, Univ. Paris-Saclay
40 rue du Pelvoux, Courcouronnes 91020 Evry, France

E-mail: f.joly@iut.univ-evry.fr
yassine.rouizi@univ-evry.fr
b.gaume@iut.univ-evry.fr
o.quemener@iut.univ-evry.fr

Abstract. In the second part of this lecture, the special case of modal reduction is discussed. This method allows to greatly reduce the size of the model in case of complex geometry. The principle of this technique is presented. A focus on the AROMM method is carried out. We insist on the necessity to choose a modal basis adapted to the physical problem. The different principles of bases reduction are introduced.

Scope

1 Introduction

As computer hardware developing, the requirements in respect of numerical simulation follow the same pattern. They are therefore becoming more demanding.
First, one have to use geometries that perfectly match the reality of the simulated object. A recent study [4] has shown that the exact numerical modelling of a simple electronic component needs a mesh of $422k$ nodes. This order of magnitude has to be compared to industrial demand, that is to obtain the simulation of an entire electronic card.
Furthermore, we are also looking for being more and more precise taking into account physical phenomena. In thermal problems, infrared radiations for example, hugely complicate the heat transfer simulations [3].
Considering the inverse approach, this effect is amplified by the iterative procedure which involve the use of an important number of simulations [1].
For all those reasons, the use of reduced models is a topical issue. The idea consist in searching the temperature field as a whole by using a small number of unknowns.

2 Context of the study: the heat equation

The problem is the following: the domain Ω, delimited by boundary Γ, is characterized by its thermal conductivity $k(M,t)$ [W.m^{-1}.K^{-1}] and its volumetric heat capacity $c(M,t)$[J.m^{-3}.K^{-1}]. This domain receives two types of thermal loadings:

- the influence of the environment, which is characterised by a temperature $T_f(M,t)\,[K]$ and a heat exchange coefficient $h(M,t)$[W.m^{-2}.K^{-1}],
- the thermal dissipation, which can be a volumetric power on the domain $\pi(M,t)$[W.m^{-3}] or a surface load on the border $\varphi(M,t)$[W.m^{-2}].

Such a problem corresponds to the following equations:

$$\left\{\begin{array}{lcl} \forall M\in\Omega & : & c\dfrac{\partial T}{\partial t} = \overrightarrow{\nabla}.(k\overrightarrow{\nabla}T)+\pi \\ \forall M\in\Gamma & : & k\overrightarrow{\nabla}T.\overrightarrow{n} = \varphi + h(T_f - T) \end{array}\right. \tag{1}$$

For complex geometries, the solution of this problem is numerical and needs a spatial discretization. The finite element method leads to the weak variational formulation of (1). Let g be the test function, defined on the Hilbert space $H^1(\Omega)$, we can write:

$$\begin{array}{rcl} \forall g\in H^1(\Omega), \quad \displaystyle\int_\Omega g\,c\,\frac{\partial T}{\partial t}\,d\Omega = & - \displaystyle\int_\Omega k\overrightarrow{\nabla}g.\overrightarrow{\nabla}T\,d\Omega - \int_\Gamma g\,h\,T\,d\Gamma \\ & + \displaystyle\int_\Omega g\,\pi\,d\Omega + \int_\Gamma g\,(\varphi + h\,T_f)\,d\Gamma \end{array} \tag{2}$$

It should be noted that it would be possible to consider:

- an anisotropic thermal conductivity characterized by a tensor $\overline{\overline{\mathbf{k}}}$,
- an advection - conduction problem, for which we add to the heat equation a transport term,
- infrared radiation between boundaries.

[1] In case of linear inverse problem, even if it is possible to use a direct procedure, this one needs one matrix inversion.

The addition of these terms does not change anything for the reduction method, and we will consider afterwards the problem defined by (1).
The spatial discretization of (2) leads to the following equation (according to the order of terms) :

$$\mathbf{C}\frac{d\mathbf{T}}{dt} = \mathbf{A}\mathbf{T} + \mathbf{U} \tag{3}$$

where $\mathbf{C}$ et $\mathbf{A}$ are respectively named the capacity matrix and the conductivity matrix, with a dimension $[N \times N]$, where N is the degrees of freedom (DOF) for the considered discretized domain. $\mathbf{T}$ is the temperature vector, which depends on the time, and $\mathbf{U}$ is the load vector. The dimension of all these vectors are $[N \times 1]$.
This equation constitutes the complete heat problem, which the DOF can be very important[2] in case of complex geometry.

3 The modal reduced model principle

This method is based on the time-space separation:

$$T(M,t) = \sum_{i=1}^{\infty} V_i(M)\, x_i(t) \tag{4}$$

Considering the space function $V_i(M)$ as being known, it means that the calculation of the temperature fields correspond to compute excitation states $x_i(t)$ of these functions. It is important to notice that the relation (4) is true only if the space functions $V_i(M)$ constitute a basis of the solutions space of the thermal problem (2), and this is not systematic.
The idea is then to rewrite this formulation using a limited number n of space functions $\widetilde{V}_i(M)$, which leads to an acceptable reconstitution of the thermal fields $\widetilde{T}(M,t) \simeq T(M,t)$:

$$\widetilde{T}(M,t) = \sum_{i=1}^{n} \widetilde{V}_i(M)\, \widetilde{x}_i(t) \tag{5}$$

Whatever the reduction technique used, the reduced model is obtained by projection of the heat equation on the subspace defined by the space functions $V_i(M)$. The equation (2) then becomes :

$$\begin{aligned} &\forall g \in H^1(\Omega), \\ &\int_\Omega g\, c\, \frac{\partial}{\partial t}\left(\sum_{i=1}^{n} \widetilde{V}_i\, \widetilde{x}_i\right) d\Omega = \\ &\qquad -\int_\Omega k \overrightarrow{\nabla} g . \overrightarrow{\nabla}\left(\sum_{i=1}^{n} \widetilde{V}_i\, \widetilde{x}_i\right) d\Omega - \int_\Gamma g\, h \left(\sum_{i=1}^{n} \widetilde{V}_i\, \widetilde{x}_i\right) d\Gamma \\ &\qquad +\int_\Omega g\, \pi\, d\Omega + \int_\Gamma g\, (\varphi + hT_f)\, d\Gamma \end{aligned} \tag{6}$$

In considering that all the space functions $\widetilde{V}_i(M)$ form a basis for the physical problem, these functions can be used as test functions for the variational formulation: $g(M) = \widetilde{V}_j(M)$.
After rearrangement, we have:

[2] For a finite volume method or for the finite element method for which the interpolation functions are linear, the DOF corresponds to the N number of mesh nodes.

$$\begin{aligned}
&\forall\ \widetilde{V}_j \in H^1(\Omega), j \in \mathbb{N}, \\
&\quad \sum_{i=1}^{n} \left(\int_\Omega \widetilde{V}_j\ c\ \widetilde{V}_i\, d\Omega \right)\ \frac{d\widetilde{x}_i}{dt} = \\
&\qquad -\sum_{i=1}^{n} \left(\int_\Omega k \overrightarrow{\nabla} \widetilde{V}_j . \overrightarrow{\nabla} \widetilde{V}_i\, d\Omega + \int_\Gamma \widetilde{V}_j\, h\, \widetilde{V}_i\, d\Gamma + \right)\ \widetilde{x}_i \\
&\qquad + \int_\Omega \widetilde{V}_j\, \pi\, d\Omega\ + \int_\Gamma \widetilde{V}_j\, (\varphi + hT_f)\, d\Gamma
\end{aligned} \tag{7}$$

After the spatial discretization, the function $\widetilde{V}_i(M)$ becomes a vector $\widetilde{\mathbf{V}}_i\,[N,1]$ resulting in:

$$\forall\ j \in [1:n], \quad \sum_{i=1}^{n} \widetilde{\mathbf{V}}_j^{\ t}\ \mathbf{C}\ \widetilde{\mathbf{V}}_i\ \frac{d\widetilde{x}_i}{dt} = -\sum_{i=1}^{n} \widetilde{\mathbf{V}}_j^{\ t}\ \mathbf{A} \widetilde{\mathbf{V}}_i\ \widetilde{x}_i + \widetilde{\mathbf{V}}_j^{\ t}\ \mathbf{U} \tag{8}$$

We name $\widetilde{\mathbf{V}}[N,n]$ the matrix which gathers the n discretized functions $\widetilde{V}_i[N,1]$, and $\widetilde{\mathbf{X}}(t)[n,1]$ the vector of the n time-dependant excitation states $\widetilde{x}_i(t)$ associated with these space functions:

$$\widetilde{\mathbf{V}}^{\ t}\ \mathbf{C}\ \widetilde{\mathbf{V}}\ \frac{d\widetilde{\mathbf{X}}}{dt} = \widetilde{\mathbf{V}}^{\ t}\ \mathbf{A}\ \widetilde{\mathbf{V}}\ \widetilde{\mathbf{X}} + \widetilde{\mathbf{V}}^{\ t}\ \mathbf{U} \tag{9}$$

Under compact form:

$$\mathbf{L}\ \frac{d\widetilde{\mathbf{X}}}{dt} = \mathbf{M}\ \widetilde{\mathbf{X}} + \mathbf{N} \tag{10}$$

with $\mathbf{L} = \widetilde{\mathbf{V}}^{\ t}\ \mathbf{C}\ \widetilde{\mathbf{V}}$ and $\mathbf{M} = \widetilde{\mathbf{V}}^{\ t}\ \mathbf{A}\ \widetilde{\mathbf{V}}$ whose dimensions are $[n,n]$, and $\mathbf{N} = \widetilde{\mathbf{V}}^{\ t}\ \mathbf{U}\ [n,1]$.

This formulation leads to the reduction of the DOF, because the complete model (2) is characterized by N unknowns, while the dimension of this modal model (10) corresponds to the n space functions $\widetilde{V}_i(M)$.

From this formulation, different methods exist to reduce a model:

- The principle of the POD (*Proper Orthogonal Decomposition*) is the identification of the space functions $\widetilde{V}_i(M)$ from several reference temperature fields (noted $T_{ref}(M,t)$ for a thermal problem). This technique has been used in a lot of studies [5, 6, 7, 8, 9, 10, 11, 12].
- The MIM (*Modal Identification Method*) is based on the direct identification of the state equation providing with the modal formulation (10) from simulations or measures. This technique has been widely used for inverse problems [13, 14, 15, 16, 13, 17, 18].
- the PGD (*Proper Generalized decomposition*) is a generalization of the decomposition principle: the temperature is written as a multiple product of a set of functions, where each of these functions depends on one variable (time, space) or one parameter (heat capacity,thermal conductivity,...). These functions are computed in enriching the basis at each iteration [19, 20, 21, 22].

- The AROMM method follows both steps which appear in the modal principle, that is:
  - to compute a complete basis $\{V_i(M)\}_{i\in\mathbb{N}}$, on which it is possible to proceed to a rigorous decomposition of the thermal fields:

$$T(M,t) = \sum_{i=1}^{\infty} V_i(M)\, x_i(t) \tag{11}$$

  - to obtain a reduced basis $\{\tilde{V}_i(M)\}_{i\in[1,n]}$, in order to decrease the model order[3], and which allows to obtain a satisfactory estimation of the thermal field :

$$T(M,t) \simeq \sum_{i=1}^{n} \widetilde{V}_i(M)\, \widetilde{x}_i(t) \tag{12}$$

The goal of this lecture consists in presenting this method.

4 The complete basis computation

We search a set of spatial functions which form a basis for the considered thermal problem (11). This set depends on the solutions space.

4.1 Classical basis

4.1.1 The Fourier basis

We consider the following thermal problem, characterized by homogeneous boundary conditions:

$$\begin{cases} \forall M \in \Omega & : \quad c_0 \dfrac{\partial T}{\partial t} = \overrightarrow{\nabla}(k_0 \overrightarrow{\nabla} T) + \pi \\ \forall M \in \Gamma & : \quad k_0 \overrightarrow{\nabla} T.\overrightarrow{n} = -h_0\, T \end{cases} \tag{13}$$

The physical parameters (heat capacity c_0, thermal conductivity k_0, and global heat exchange coefficient h_0) are limited to spatial functions.
The space functions $\hat{V}_i^F(M)$ correspond to eigenvectors and are obtained by the resolution of the eigenvalues problem associated to the physical problem:

$$\begin{cases} \forall M \in \Omega & : \quad \overrightarrow{\nabla}\left(k_0 \overrightarrow{\nabla} \hat{V}_i^F\right) = z_i^F\, c_0\, \hat{V}_i^F \\ \forall M \in \Gamma & : \quad k_0 \overrightarrow{\nabla} \hat{V}_i.\overrightarrow{n} = -h_0\, \hat{V}_F \end{cases} \tag{14}$$

z_i^F [s^{-1}] is the eigenvalue associated to each eigenvector $\hat{V}_i^F$. The inverse of this quantity is a time τ_i^F [s] named the time constant of the eigenvector. It characterizes the dynamic of the eigenmode:

$$\tau_i^F = \frac{-1}{z_i^F} \tag{15}$$

These Fourier eigenmodes (Figure 1.a) can be considered as particular temperature fields: the eigenvalues problem corresponds to a stationary physical problem with a volumetric thermal load which is proportional to the eigenmode searched at each point of the domain, and whose boundary conditions are homogeneous.

[3] As we'll see later, the reduced function $\tilde{V}_i(M)$ do not correspond necessary with the functions $V_i(M)$ of the complete basis. This explains the change of notation

The variational form of the eigenvalues problem is :

$$\forall g \in H^1(\Omega), \quad -\int_\Omega k_0 \overrightarrow{\nabla} g \,.\, \overrightarrow{\nabla} \hat{V}_j^F \, \partial\Omega - \int_\Gamma g \, h_0 \, \hat{V}_i^F = z_i^F \int_\Omega g \, c_0 \, \hat{V}_i^F \, \partial\Omega \tag{16}$$

In cases of complex geometries, such eigenvalues problem is solved numerically, from a spatial discretization characterized by N DOF. The number of eigenmodes becomes then finite and equal to N. The numerical resolution is performed by the Lanczos method [23], from the discrete formulation of (16). In using the same matrix than specified previously (3), we have:

$$\mathbf{A} \; \hat{\mathbf{V}}_i^F = z_i^F \; \mathbf{C} \; \hat{\mathbf{V}}_i^F \tag{17}$$

This method had been implemented in all principal languages (Matlab since 1996 [24], Arpack since 1998 [25]). It allows to compute the eigenmodes according to the order of the most important time constants τ_i^F.

The set of all the eigenmodes $\hat{V}_i^F$ form a basis for the subspace $H_F^1(\Omega) \subset H^1(\Omega)$, which corresponds to this of the physical problem (13).

The eigenmodes are mutually-orthogonal according to a scalar product $< u, v >= \int_\Omega u c v \, \partial\Omega$:

$$\forall i \neq j, \quad < \hat{V}_i^F, \hat{V}_i^F >= \int_\Omega \hat{V}_i^F \, c_0 \, \hat{V}_j^F \, \partial\Omega = 0 \tag{18}$$

A standardization allows to impose the magnitude of each mode. In choosing:

$$V_i^F = \frac{\hat{V}_i^F}{\left(\int_\Omega \hat{V}_i^F \, c_0 \, \hat{V}_i^F \, d\Omega \right)^{1/2}} \tag{19}$$

we obtain the first orthogonality property:

$$\forall i, j \in \mathbb{N}, \quad < V_i^F, V_j^F >= \int_\Omega V_i^F \, c_0 \, V_j^F \, \partial\Omega = \delta_{ij} \tag{20}$$

Because of (16), and in choosing the eigenmodes V_j^F as test function, we have:

$$-\int_\Omega k_0 \overrightarrow{\nabla} V_i^F \,.\, \overrightarrow{\nabla} V_j^F \, d\Omega - \int_\Gamma V_i^F \, h_0 \, V_j^F \, d\Gamma = z_i^F \int_\Omega V_i^F \, c_0 \, V_j^F d\Omega \tag{21}$$

The use of the first orthogonality property (20) enables finally to obtain the second orthogonality property:

$$-\int_\Omega k_0 \overrightarrow{\nabla} V_i^F \,.\, \overrightarrow{\nabla} V_j^F \, d\Omega - \int_\Gamma V_i^F \, h_0 \, V_j^F \, d\Gamma = z_i^F \, \delta_{ij} \tag{22}$$

We saw previously that the state equation has been obtained by the projection of the thermal problem on the reduced basis (eq. (7)).
In the case where all the complete basis $\left(z_i^F \, , \, V_i^F \right)$ is used, we obtain:

$$\begin{aligned} &\forall \, j \in \mathbb{N}, \\ &\sum_{i=1}^{n} \left(\int_\Omega V_j^F \;\; c_0 \;\; V_i^F \, d\Omega \right) \;\; \frac{\partial x_i}{dt} = \\ &\qquad + \sum_{i=1}^{n} \left(\int_\Omega k_0 \overrightarrow{\nabla} V_j^F . \overrightarrow{\nabla} V_i^F \, \partial\Omega \int_\Gamma V_j^F \, h_0 \, V_i^F \, \partial\Gamma + \right) \;\; x_i \\ &\qquad + \int_\Omega \pi \, V_j^F \, \partial\Omega \end{aligned} \tag{23}$$

Because of the orthogonality properties (eq. (20) et (22)), all the state equations are fully decoupled:

$$\forall\, j \in \mathbb{N}, \quad \frac{\partial x_j}{\partial t} = z_j^F\, x_j + \int_\Omega V_j^F\, \pi\, \partial\Omega \tag{24}$$

As we will see later, the reduced basis $\left(\tilde{z}_i^F\ ,\ \tilde{V}_i^F\right)$ from his complete basis $\left(z_i^F\ ,\ V_i^F\right)$ is built, such as these previous orthogonality properties (eq. (20) et (22)) are preserved. The decoupled state-reduced equations (24) allow to obtain an immediate resolution.
The Fourier basis is valid for a linear thermal problem, with stationary parameters and with homogeneous boundary conditions, whatever the value of the thermal exchange coefficient $h_0(M)$.

In the particular case where $\forall M \in \Gamma, h_0 = 0$, we have the Neumann problem :

$$\begin{cases} \forall M \in \Omega & : \quad c_0 \dfrac{\partial T}{\partial t} = \overrightarrow{\nabla}(k_0 \overrightarrow{\nabla} T) + \pi \\ \forall M \in \Gamma & : \quad \overrightarrow{\nabla} T . \overrightarrow{n} = 0 \end{cases} \tag{25}$$

The eigenvalues problem associated is then the Neumann eigenvalues problem :

$$\begin{cases} \forall M \in \Omega & : \quad \overrightarrow{\nabla}\left(k_0 \overrightarrow{\nabla} \hat{V}_i^N\right) = z_i^N\, c_0\, \hat{V}_i^N \\ \forall M \in \Gamma & : \quad \overrightarrow{\nabla} \hat{V}_i^N\, .\, \overrightarrow{n} = 0 \end{cases} \tag{26}$$

This set of eigenvectors $\hat{V}_i^N$ forms a basis for the subspace $H_N^1(\Omega) \subset H^1(\Omega)$. Then they are characterized by a zero heat flux on the boundaries (Figure 1.b).

4.1.2 The Dirichlet basis

We consider a Dirichlet problem characterized by the following equations [4]:

$$\begin{cases} \forall M \in \Omega & : \quad c_0 \dfrac{\partial T}{\partial t} = \overrightarrow{\nabla}.(k_0 \overrightarrow{\nabla} T) + \pi \\ \forall M \in \Gamma & : \quad T = 0 \end{cases} \tag{27}$$

This problem defines a particular space of solutions named Dirichlet space H_0^1. It is a subspace of the Hilbert space H^1, which respects the boundary condition.

Eigenvectors $\hat{V}_i^D(M)$ are obtained by the resolution of the following eigenmodes problem :

$$\begin{cases} \forall M \in \Omega & : \quad \overrightarrow{\nabla}\left(k_0 \overrightarrow{\nabla} \hat{V}_i^D\right) = z_i^D\, c_0\, \hat{V}_i^D \\ \forall M \in \Gamma & : \quad \hat{V}_i^D = 0 \end{cases} \tag{28}$$

The variational form is as follows[5]:

[4] In practical terms, it is numerically possible to approach a Dirichlet thermal problem by a general Fourier formulation, in which we fix $h_0 \to \infty$. It is the same for the associated Dirichlet eigenvalues problem. Even if mathematical proof needs a rigorous writing of the problem (equations (27) and (28)), using such an expression for a numerical approach gives good results.

[5] One use here a test function $g \in H_0^1(\Omega)$, which has then a zero value on the boundaries. The integral term $\int_\Gamma g\, k\, \overrightarrow{\nabla} \hat{V}_i^D . \overrightarrow{n}\, d\Gamma$ is then a zero value.

$$\forall g \in H_0^1(\Omega), \quad -\int_\Omega k_0 \overrightarrow{\nabla} g \,.\, \overrightarrow{\nabla} \hat{V}_j^D \, \partial\Omega = z_i \int_\Omega g \, c_0 \, \hat{V}_i^D \, \partial\Omega \tag{29}$$

This set of all the eigenvectors V_i^D forms a basis for the Dirichlet subspace $H_0^1(\Omega) \subset H^1(\Omega)$. Then they are characterized by a zero value on the boundaries, as shown in figure (1.c).

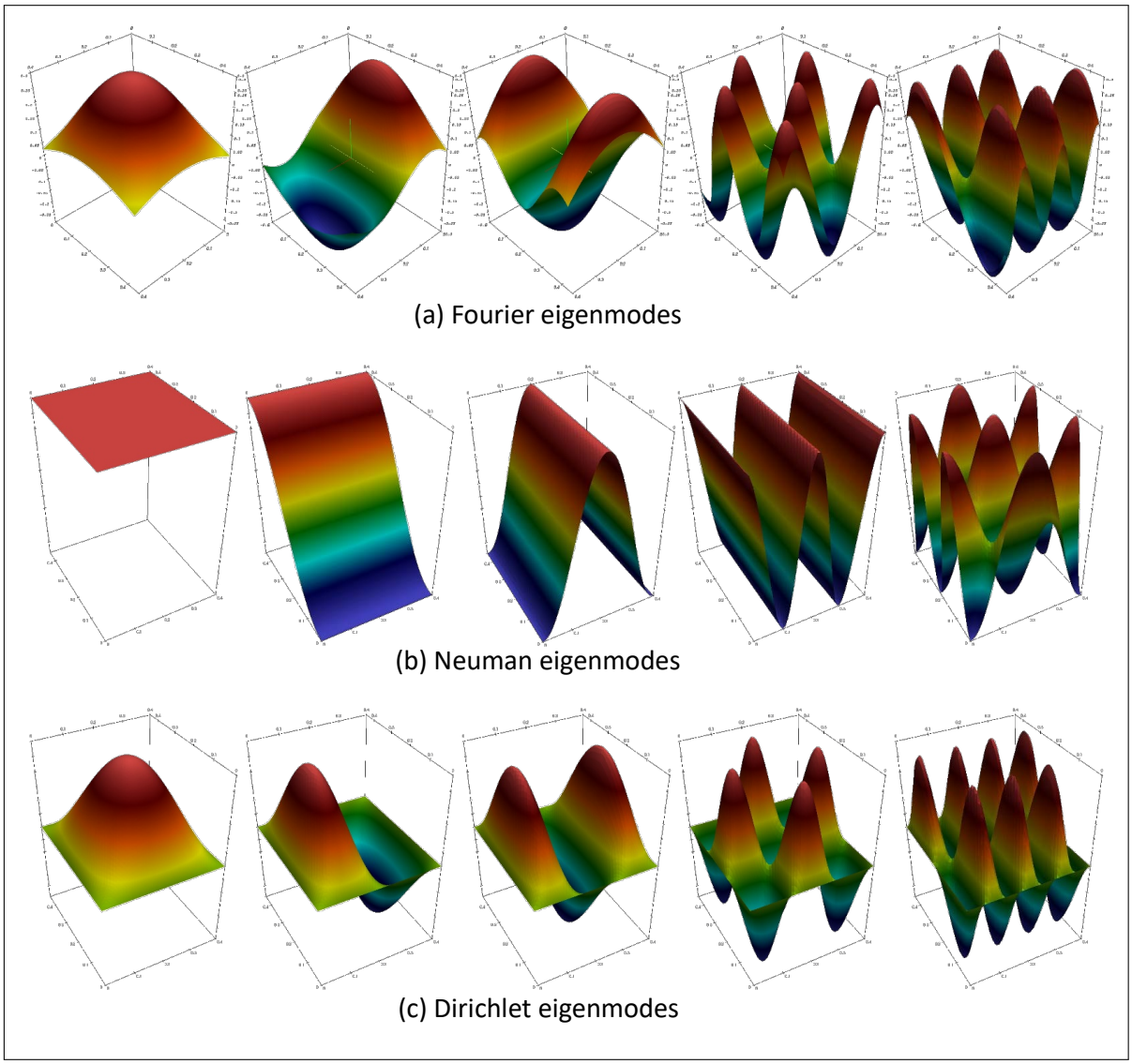

Figure 1: Classical modes for a simple 2D rectangular geometry

An adapted normalization[6] enables to fix the magnitude of the modes, and leads to the following orthogonality relations:

$$\forall i,j \in \mathbb{N}, \begin{cases} \int_\Omega V_i^D \, c_0 \, V_j^D \, \partial\Omega = \delta_{ij} \\ \int_\Omega k_0 \overrightarrow{\nabla} V_i^D \, . \, \overrightarrow{\nabla} V_j^D \, d\Omega = z_i^D \, \delta_{ij} \end{cases} \tag{30}$$

4.1.3 Non homogeneous problem: applying a gliding temperature

We consider the general problem for which we recall the equations:

$$\begin{cases} \forall M \in \Omega & : & c_0 \dfrac{\partial T}{\partial t} = \overrightarrow{\nabla}(k_0 \overrightarrow{\nabla} T) + \pi \\ \forall M \in \Gamma & : & k_0 \overrightarrow{\nabla} T . \overrightarrow{n} = \varphi + h_0 (T_f - T) \end{cases} \tag{31}$$

We saw that the Fourier eigenmodes (14) form a basis for a thermal problem characterized by homogeneous boundary conditions. In order to use the modal reduction with theses eigenmodes, we have to split the temperature T on two terms :

$$T = T_g + T_d \tag{32}$$

- The term T_g is called the gliding temperature, because it corresponds to the temperature obtained without any consideration of the thermal inertia:

$$\begin{cases} \forall M \in \Omega & : & 0 = \overrightarrow{\nabla}(k_0 \overrightarrow{\nabla} T_g) + \pi \\ \forall M \in \Gamma & : & k_0 \overrightarrow{\nabla} T_g . \overrightarrow{n} = \varphi + h_0 (T_f - T_g) \end{cases} \tag{33}$$

  Such a problem is simple: from the variationnal formulation from (33):

$$-\int_\Omega k_0 \overrightarrow{\nabla} g \, . \, \overrightarrow{\nabla} T_g \, d\Omega - \int_\Gamma g \, h_0 \, T_g \, d\Gamma + \int_\Omega g \, \pi \, d\Omega + \int_\Gamma g \, (\varphi + h_0 \, T_f) \, d\Gamma = 0 \tag{34}$$

  the discrete form is then:

$$\mathbf{A T_g} + \mathbf{U}(t) = 0 \tag{35}$$

  and we have then:

$$\mathbf{T_g} = -\mathbf{A}^{-1} \mathbf{U}(t) \tag{36}$$

- The complementary variable T_d is called the dynamic temperature. From (31) and (33), the equation which allows to obtain T_d is :

$$\begin{cases} \forall M \in \Omega & : & c_0 \dfrac{\partial T_d}{\partial t} = \overrightarrow{\nabla}(k_0 \overrightarrow{\nabla} T_d) - c_0 \dfrac{\partial T_g}{\partial t} \\ \forall M \in \Gamma & : & k_0 \overrightarrow{\nabla} T_d . \overrightarrow{n} = -h_0 \, T_d \end{cases} \tag{37}$$

  Such problem is then homogeneous and it is then allowed to reduce it by using the Fourier basis.

Lastly the researched temperature field T is:

$$T = \sum_{i=1}^{\infty} x_i \, V_i^F + T_g \tag{38}$$

[6] It is the same as the one used for the Fourier eigenmodes (eq. (19))

The state modal problem is always decoupled. The gliding temperature T_g appears only in cases of time variation of the solicitations:

$$\forall(i) \in \mathbb{N}, \quad \frac{dx_i}{dt} = z_i\, x_i - \int_\Omega V_i^F\, c_0 \frac{dT_g}{dt} d\Omega \tag{39}$$

Several studies have used this technique, including buildings problems [26, 27, 28, 29].

Hovewer, the limit of this method is that the computed basis is applicable only for problems in which the boundary conditions are fixed. From the second equation of (14), we can define the quantity γ_i such as:

$$\gamma_i = \frac{\overrightarrow{\nabla} V_i . \overrightarrow{n}}{V_i} = \frac{-h_0}{k_0} \tag{40}$$

In this way we can see that all the eigenvectors are characterized by the same value of this quantity γ_i. Thus, all the dynamic thermal fields that can be rebuilt by this modal formulation have to respect this constraint.
Such basis are not compatible with a thermal problem in which non linearities or time variations exist on the boundaries. Examples are numerous: time dependant exchange coefficient $h(t)$, thermal conductivity depending on the temperature $k(T)$, infrared radiations... That is why other basis have been developed.

4.2 Basis adapted to non linear problems

4.2.1 Branch modes

In order to avoid this limit, a new basis is defined, whose boundary conditions are not linked with the physical boundary conditions:

$$\begin{cases} \forall M \in \Omega \quad , \quad k_0 \overrightarrow{\nabla}(\overrightarrow{\nabla} \hat{V}_i^B) = z_i^B\, c_0\, \hat{V}_i^B \\ \forall M \in \Gamma \quad , \quad k_0 \overrightarrow{\nabla} \hat{V}_i^B . \overrightarrow{n} = -z_i^B\, \zeta\, \hat{V}_i^B \end{cases} \tag{41}$$

The feature of this basis is that the eigenvalues z_i^B is present in the boundary condition. This is the Steklov condition.
The quantity ζ [J.m^{-2}K^{-1}] is called Steklov parameter and it is a simple coefficient which allows to respect the physical dimensions in the boundary condition equations. The value of this coefficient is obtained from the variational formulation of the eigenvalues problem (41).

$$-\int_\Omega k_0 \overrightarrow{\nabla} g . \overrightarrow{\nabla} V_i^B\, d\Omega = z_i \left(\int_\Omega c_0\, g\, V_i^B\, d\Omega + \int_\Gamma \zeta\, g\, V_i^B\, d\Gamma \right) \tag{42}$$

To balance the two terms linked to the eigenvalue, an appropriate choice of the Steklov coefficient ζ is given by:

$$\zeta \simeq \frac{\int_\Omega c_0\, d\Omega}{\int_\Gamma d\Gamma} \tag{43}$$

In using the associated scalar product:

$$< u, v >= \int_\Omega u\, c_0\, v\, d\Omega + \int_\Gamma u\, \zeta\, v\, d\Gamma \tag{44}$$

the normalisation is done:

$$V_i^B = \frac{\hat{V}_i^B}{\left(\int_\Omega \hat{V}_i^B \, c_0 \, \hat{V}_i^B \, d\Omega + \int_\Gamma \hat{V}_i^B \, \zeta \, \hat{V}_i^B \, d\Gamma\right)^{1/2}} \tag{45}$$

and we obtain the following orthogonality properties:

$$\begin{aligned} &\forall (i,j) \in \mathbb{N}^2, \\ &\int_\Omega V_j^B \, c_0 \, V_i^B \, d\Omega + \int_\Gamma V_i^B \, \zeta \, V_i^B \, d\Gamma = \delta_{ij} \\ &\int_\Omega k_0 \overrightarrow{\nabla} V_j^B \, . \, \overrightarrow{\nabla} \, V_i^B \, d\Omega = z_i^B \, \delta_{ij} \end{aligned} \tag{46}$$

It is possible to characterize the spatial evolution of each Branch modes by defining a form coefficient C_i^ζ for each mode V_i^B:

$$C_i^\zeta = \int_\Gamma V_i^B \, \zeta \, V_i^B \, d\Gamma \tag{47}$$

The evolution of this coefficient according to the mode number, for a simple rectangular geometry, is presented on figure 2. It shows that two Branch modes families exist:

- Because of the orthogonality relation defined in Eq. (14), when C_i^ζ is close to 1, the considered mode is flat on the domain except near the border. Such modes are called Boundary modes. They do not appear in a classical Fourier basis, and allow the reconstitution of any boundary conditions.
- There exist others modes for which the spatial evolutions are located in all the domain. We call them Domain modes. These modes are characterized by a weak value of c_i^ζ (less than 0.3 for the example in figure 2). These are less numerous as the Boundaries modes (for the first computed modes).

Figure 3.a represents some Branch modes for a simple 2D rectangular geometry. This figure enables to clearly visualize these two families of Branch modes.

With these Branch modes, the orthogonality properties don't allow anymore to obtain a decoupled modal problem:

$$\begin{aligned} \forall j \in \mathbb{N}, \quad &\sum_{i=1}^{\infty} \left(\int_\Omega V_j^B \, c \, V_i^B \, d\Omega \right) \frac{dx_i}{dt} \\ &= \sum_{i=1}^{\infty} \left(\int_\Omega k \overrightarrow{\nabla} V_j^B \, . \overrightarrow{\nabla} V_i^B \, d\Omega + \int_\Gamma V_j^B \, h \, V_i^B \, d\Gamma \right) x_i \\ &+ \int_\Omega V_j^B \, \pi \, d\Omega + \int_\Gamma V_j^B \, (hT_e + \varphi) d\Gamma \end{aligned} \tag{48}$$

This is the price to pay for using this Branch basis.

On the other hand, the Branch modes form a basis for any thermal problem, including those characterized by parameters that are functions of time or temperature. One shows that the generated functionnal space is the Hilbert space $H^1(\Omega)$ and we have directly[7]:

[7] It is no longer necessary to use the sliding temperature field

$$T(M,t) = \sum_{i=1}^{\infty} x_i \, V_i^B \tag{49}$$

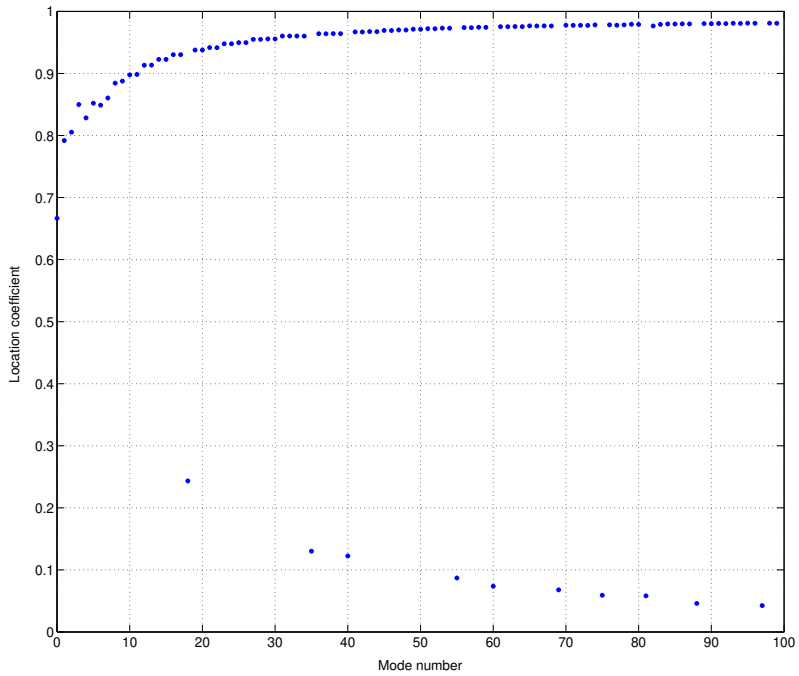

Figure 2: Evolution of the location coefficient according to the branch mode number

Initiated by Neveu *et al.* [30], this base type has been applied to different configurations: Quéméner *et al.* [31] treats the case of a non-linear problem, with the existence of solidification of a molded part. Various applications are made for inverse problems by Videcoq *et al.* [32, 33, 34]. Branch bases generalized to problems of diffusion with transport are proposed by Joly *et al.* [35], then used in the case of an inverse problem of identification [36]. Finally Laffay *et al.* [37, 38] proposes a substructuring technique, which allows the computation of Branch bases for different subdomains, which are then coupled each other by a thermal contact resistance.

4.2.2 The Dirichlet-Steklov eigenmodes

Recently another way to reduce non linear problems with or without time dependant parameters has been developped. It consist in using two bases:

- the Dirichlet basis seen previously (eq. (27)),
- the Steklov basis[8], which is defined by the following eigenvalues problem:

$$\begin{cases} \forall M \in \Omega \quad , \quad \overrightarrow{\nabla}(k_0 \overrightarrow{\nabla} \hat{V}_i^S) = 0 \\ \forall M \in \Gamma \quad , \quad k_0 \overrightarrow{\nabla} \hat{V}_i^S . \overrightarrow{n} = -z_i^S \, \zeta \, \hat{V}_i^S \end{cases} \tag{50}$$

Steklov modes correspond to stationary fields obtained for a problem in which one imposes fluxes at the boundaries, whose value is proportional to the value of this mode at

[8] Steklov modes are rigorously defined only on the boundaries. In order to simply the notation, we call here by abuse of language the steklov mode as their extension in the domain (noted $\hat{V}_i^S$)

any point on the border.

The regrouping of these two families of modes $\{V_i^D\}_{i\in\mathbb{N}} \bigoplus \{V_j^S\}_{j\in\mathbb{N}}$ forms a hilberian basis de $H^1(\Omega)$.
We define the following scalar product:

$$< u, v >= \int_\Omega k_0 \overrightarrow{\nabla} u \ . \ \overrightarrow{\nabla} v \, d\Omega + z_0 \int_\Gamma u \, \zeta \, v \, d\Gamma \tag{51}$$

where z_0 is a constant parameter $[s^{-1}]$ which allows to respect the coherence of the physical dimension of both terms.

Using the following standardization:

$$V_i^S = \frac{\hat{V}_i^{DS}}{\left(\int_\Omega k_0 \overrightarrow{\nabla} \hat{V}_i^{DS} \, . \, \overrightarrow{\nabla} \hat{V}_i^{DS} \, d\Omega + z_0 \int_\Gamma \hat{V}_i^{DS} \, \zeta \, \hat{V}_i^{DS} \, d\Gamma \right)^{1/2}} \tag{52}$$

we obtain Dirichlet and Steklov modes which are orthogonal with respect to this scalar product (51):

$$\begin{aligned} &\forall \mathcal{X}, \mathcal{Y} \in \{D, S\}, \forall i, j \in \mathbb{N}, \\ &< \hat{V}_i^{\mathcal{X}}, \hat{V}_j^{\mathcal{Y}} > \ = \int_\Omega k_0 \overrightarrow{\nabla} \hat{V}_i^{\mathcal{X}} \, . \, \overrightarrow{\nabla} \hat{V}_j^{\mathcal{Y}} \, d\Omega + z_0 \int_\Gamma \hat{V}_i^{\mathcal{X}} \, \zeta \, \hat{V}_j^{\mathcal{Y}} \, d\Gamma \\ &\qquad\qquad = \delta_{\mathcal{X}\mathcal{Y}} \, \delta_{ij} \end{aligned} \tag{53}$$

A sets of modes of the Dirichlet-Steklov basis is compared to the Branch modes in Figure 3. This shows that Steklov's modes correspond very well to Boudaries Branch modes, whereas Domain Branches modes and Dirichlet modes are similar only inside the domain. At the boundaries,the Domain Branch modes are not characterized by null values, unlike Dirichlet modes. Nevertheless the correspondence between these two bases is flagrant.

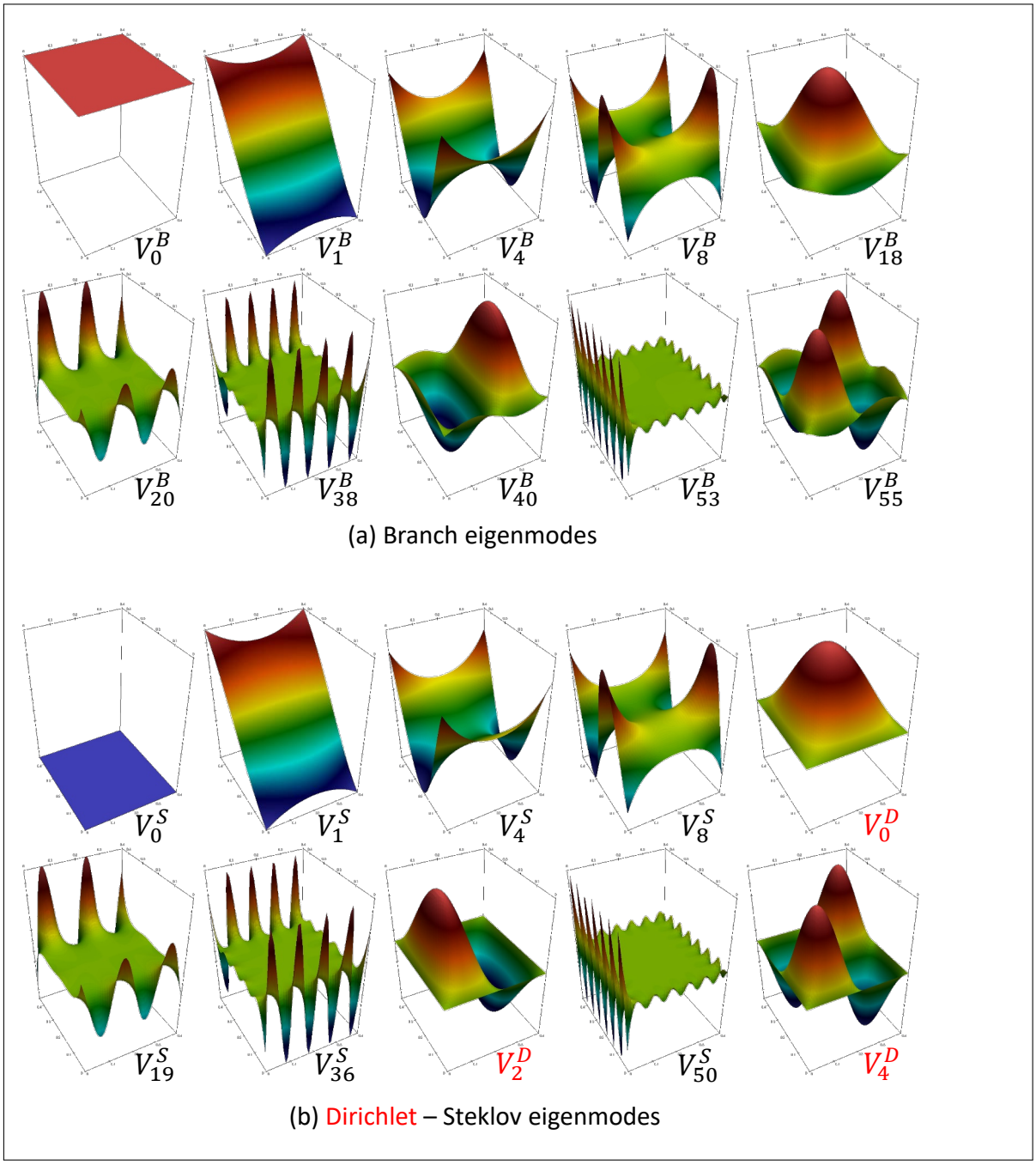

Figure 3: Comparison between the Branch basis $\{V_i^B\}$ and the Dirichlet-Steklov basis $\{V_i^D\} \bigoplus \{V_j^S\}$

5 Reducing the basis

Until now, no reduction has been made. Whatever the chosen basis, the problem of state (eq.(39) or (48)) remains characterized by a size related to spatial discretization. The second step of the AROMM method is then to build a reduced base containing n modes $\tilde{V}_i(M)$ from the complete base. We saw previously that the form of the modal problem resulting from this reduction depends on the used base:

- For a base associated with a linear thermal problem and with stationary parameters (ie Fourier base $\{V_i^F\}$, Neumann base $\{V_i^N\}$ or Dirichlet base $\{V_i^D\}$):

$$\forall i \in \{1,n\} \quad \frac{dx_i}{dt} = z_i\, x_i - \int_\Omega \tilde{V}_i\, c_0\, \frac{dT_g}{dt} d\Omega \tag{54}$$

- For a base adapted to more general problems (ie Branch base $\{V_i^B\}$ or Diriclet-Steklov base $\{V_i^D\} \bigoplus \{V_j^S\}$):

$$\begin{aligned} \forall j \in \{1,n\} \quad & \sum_{i=1}^{n} \left(\int_\Omega \tilde{V}_j\, c\, \tilde{V}_i\, d\Omega \right) \dot{x}_i \\ & = \sum_{i=1}^{n} \left(\int_\Omega k \vec{\nabla} \tilde{V}_j \,.\, \vec{\nabla} \tilde{V}_i\, d\Omega + \int_\Gamma \tilde{V}_j\, h\, \tilde{V}_i\, d\Gamma \right) x_i \\ & + \int_\Omega \tilde{V}_j\, \pi\, d\Omega + \int_\Gamma \tilde{V}_j\, (h\, T_e + \varphi)\, d\Gamma \end{aligned} \tag{55}$$

Several reduction methods exist.

5.1 Truncation

The simplest idea is to take the most relevant modes from the complete base:

$$\forall i \in \{1,n\} \quad \forall j \in \{1,N\} \quad , \quad \tilde{V}_i = V_j \tag{56}$$

5.1.1 Temporal Truncation

A first criterion leads to the truncation of Marshall [39]. In this method the modes with the largest time constants are kept. Independent of any reference problem, this reduction technique has mostly been used for classical basis [40].

An important advantage of this reduction is that it is immediate to use, since the Lanczos technique allows the base to be calculated according to the order of the largest time constants. Thus, temporal truncation can also be used as first-level reduction: instead of calculating the complete base, only a certain percentage of this base is computed, from which it is possible to make a second reduction more efficient. In the case of thermal problems characterized by a very large number of DOF, this possibility of partial calculations of the base is of great interest, given the important calculation times needed for solving the eigenvalue problem and the difficulties of the eigenvectors storage.

5.1.2 Energetic Truncation

This technique is used by Joly *et al.* [35]. From a set of known temperature fields $T_{ref}(t)$, it is possible to obtain the excitation states by a simple projection of the complete basis on

T_{ref} according to the definition of the scalar product defined for the considered basis.

For example, in the case of Branch basis, orthogonal properties lead to:

$$\begin{aligned}
&\forall j \in \mathbb{N}, \\
&\int_\Omega T_{ref}\, c_0\, V_j^B\, d\Omega + \int_\Gamma T_{ref}\, \zeta\, V_j^B\, d\Gamma \\
&\qquad = \int_\Omega \sum_{i=1}^{n} \left(x_i\, V_i^B\right) c_0\, V_j^B\, d\Omega + \int_\Gamma \sum_{i=1}^{n} \left(x_i\, V_i^B\right)\, \zeta\, V_j^B\, d\Gamma \\
&\qquad = \sum_{i=1}^{n} \left(\int_\Omega V_i^B\, c_0\, V_j^B\, d\Omega + \int_\Gamma V_i^B\, \zeta\, V_j^B\, d\Gamma \right) x_i \\
&\qquad = \sum_{i=1}^{n} \delta_{ij} x_i \\
&\qquad = x_j
\end{aligned} \tag{57}$$

For the Dirichlet Steklov basis, given the definition of the scalar product used, the projection leads to:

$$\begin{aligned}
&\forall \mathcal{X}, \mathcal{Y} \in \{D, S\}, \forall j \in \mathbb{N}, \\
&\int_\Omega k_0 \overrightarrow{\nabla} T_{ref} \,.\, \overrightarrow{\nabla} \hat{V}_j^{\mathcal{Y}}\, d\Omega + \int_\Gamma T_{ref}\, \zeta\, \hat{V}_j^{\mathcal{Y}}\, d\Gamma \\
&\qquad = \int_\Omega k_0 \overrightarrow{\nabla} \left(\sum_{i=1}^{n} x_i\, \hat{V}_i^{\mathcal{X}} \right) \,.\, \overrightarrow{\nabla} \hat{V}_j^{\mathcal{Y}}\, d\Omega + \int_\Gamma \left(\sum_{i=1}^{n} x_i\, \hat{V}_i^{\mathcal{X}} \right)\, \zeta\, \hat{V}_j^{\mathcal{Y}}\, d\Gamma \\
&\qquad = \sum_{i=1}^{n} \left(\int_\Omega k_0 \overrightarrow{\nabla} \hat{V}_i^{\mathcal{X}} \,.\, \overrightarrow{\nabla} \hat{V}_j^{\mathcal{Y}}\, d\Omega + \int_\Gamma \hat{V}_i^{\mathcal{X}}\, \zeta\, \hat{V}_j^{\mathcal{Y}}\, d\Gamma \right) x_i \\
&\qquad = \sum_{i=1}^{n} \delta_{\mathcal{X}\mathcal{Y}}\, \delta_{ij}\, x_i \\
&\qquad = x_j
\end{aligned} \tag{58}$$

The knowledge of the excitation states for all the modes of the complete basis makes it possible to keep only those characterized by the most important states for all the temperature fields used. This technique generally leads to a more efficient reduction than the simple temporal truncation, but it has a disadvantage: the effectiveness of the reduction depends on the reference fields that must be known. Here we find the same constraint as that existing for the POD method.
From the same discretized geometry it is generally possible to perform simulations of a thermal problem which is simpler than that studied, but which will however be able to excite the characteristic modes.

5.2 Amalgamated base

An even more elaborate technique is that of the amalgam. It brings back the idea of classifying the eigenmodes according to their states of excitation, but this time, the modes which are not kept during the truncation are added by simple linear combinations to the retained modes:

$$\forall i \in \{1, n\} \quad \tilde{V}_i = V_{i,1} + \sum_{p=2}^{\tilde{N}_i} \alpha_{i,p} V_{i,p} \quad ; \quad 0 < |\alpha_{i,p}| < 1 \tag{59}$$

In order to maintain the properties of the base, each mode is used only once:

$$\sum_{i=1}^{n} \left(\tilde{N}_i + 1 \right) = N \tag{60}$$

The distribution of the initial modes and the computation of the amalgam coefficient $\alpha_{i,p}$ are carried out in a fast sequential procedure which depends only on the knowledge of the excitation states. Set up by Oulefki [41] in the case of classical bases for which decoupling made it easy to determine the reference states, this reduction technique has been widely used for Branch modes.
The difficulty is in general to determine the excitation states of the complete basis. A first rather simple solution [42, 43] is, as for energetic truncation, to use a set of temperature fields obtained by complete resolution of a reference problem, which gives access to the excitation states (eq. (57) or (58)).
Other techniques have also been tested [31, 33, 37] in order to avoid computing the reference thermal fields: since the eigenmodes excitation states are known only to classify this modes in order to set up the amalgam procedure, these authors have built the associated complete modal problem, and sought a simple estimate of the states of excitation: Using a Branch basis and neglecting the terms of coupling between modes, the modal problem has been solved analytically and the excitation states became extremely fast to obtain [31]. An improvement of this technique has been carried out later in the case of a rotating disc, for which only the coupling of a small number of modes is taken into account [44].

6 Application to the inverse problems: Examples

The examples presented here concern the automobile brake system, which is a major safety component. It undergoes, during its operating phase, many mechanical and thermal stresses, which can lead to important damages: cracks, apparition of hot-judder, vapor locking, brake fade, etc.
Because of thermal solicitations are rarely known (especially the part of the heat flux received by the pad and by the disc), the inverse techniques is used. In order to respect the complex geometry of the system, the model used in the inverse process is numerical, and characterized by very fine meshes. Computing time and memory problems appear very quickly, and a solution is to use reduced models.

6.1 Estimation of heat flux received by the brake disc rotating [1]

A brake disc in rotation with variable rotation frequency $\omega(t)$ is considered (Fig. 4). During the braking phase, the disc receives a time-dependent heat flux on the zone of friction with the brake pads Ω_1. The flux density $\varphi[W.m^{-2}]$ dissipated by friction is not uniform but varies linearly with the velocity thus with the radius.
The space discretization using P1 finite elements leads to a DOF $N = 9860$ for the following matrix formulation:

$$\mathbf{C}\frac{d\mathbf{T}}{dt} = \left[\mathbf{K} + \omega_u(t)\mathbf{U} + h_u(t)\mathbf{H}\right]\mathbf{T} + \varphi_u\mathbf{U} \tag{61}$$

The goal consists in identifying $\varphi_u(t)$ in real time, from a local infrared mesurement on the disc (point A).
Concerning the direct simulation, the computing time is significant (equal to 2160 s on a simple laptop), because of the transport term which involves small computation time-steps. Figure 5 illustrates this phenomenon.
Such simulation time is an obstacle for inverse applications where the need for real-time response is important. To avoid prohibitive time, a reduced model is built. It is obtained by

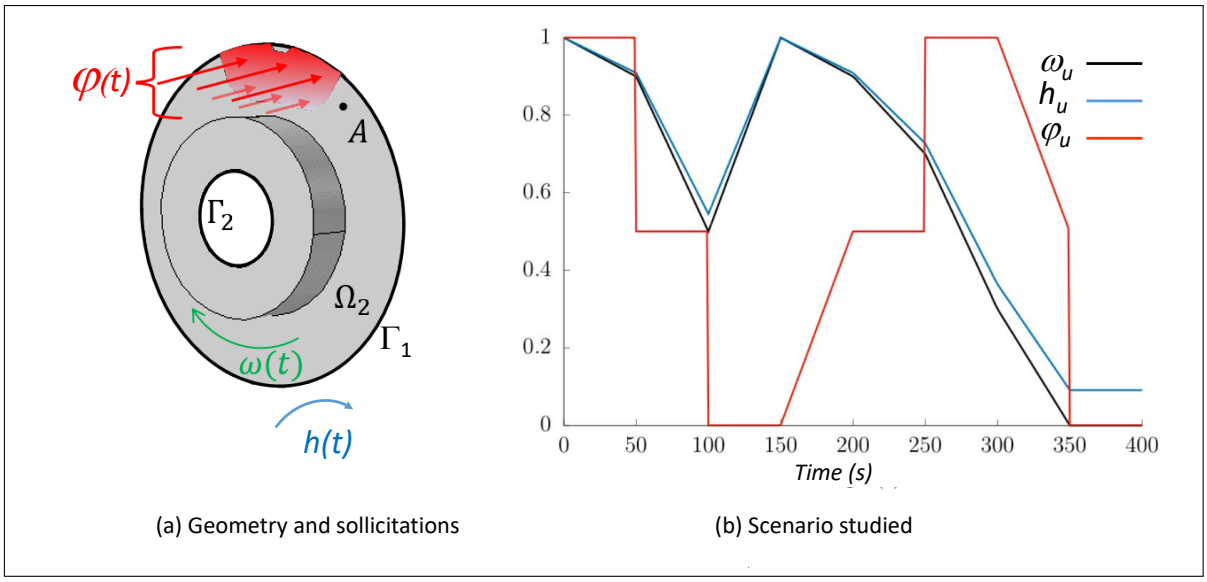

Figure 4: Physical problem

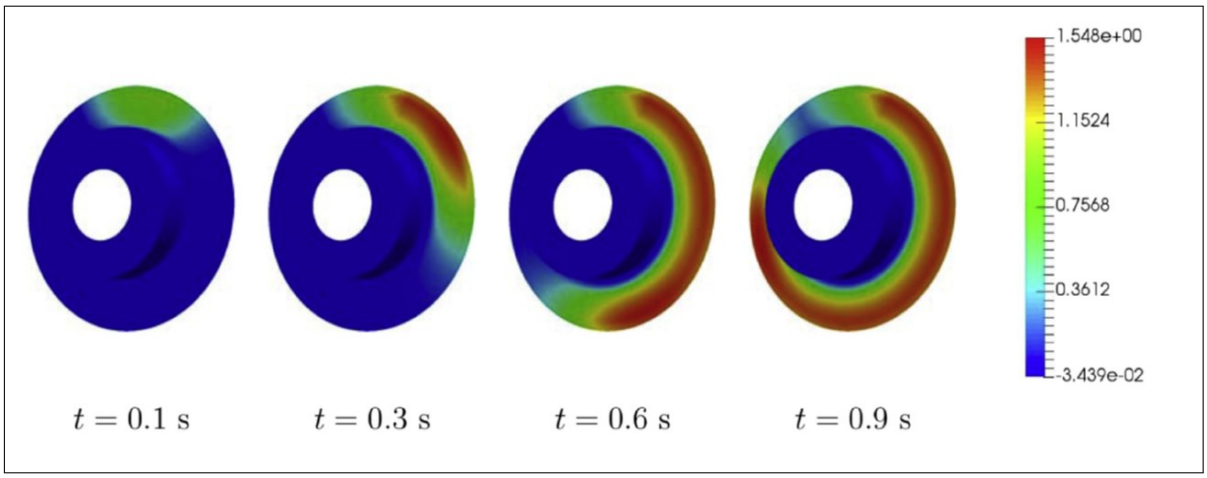

Figure 5: Temperature fields at different times

the AROMM method, in choosing Branch eigenmodes (fig 6.a) and the Amalgam method. The reference scenario used for the Amalgam procedure (fig 6.b) is obviously different from the one used for the identification (fig 4.b). With a reduced order $n = 15$, the direct simulation requires less than 10s, with satisfying results (fig 7).
By integrating such reduced model in an inverse approach, it is then possible to identify the heat flux φ in quasi real time. The inverse algorithm is based on the adjoint method applied on sliding time windows (fig 8).

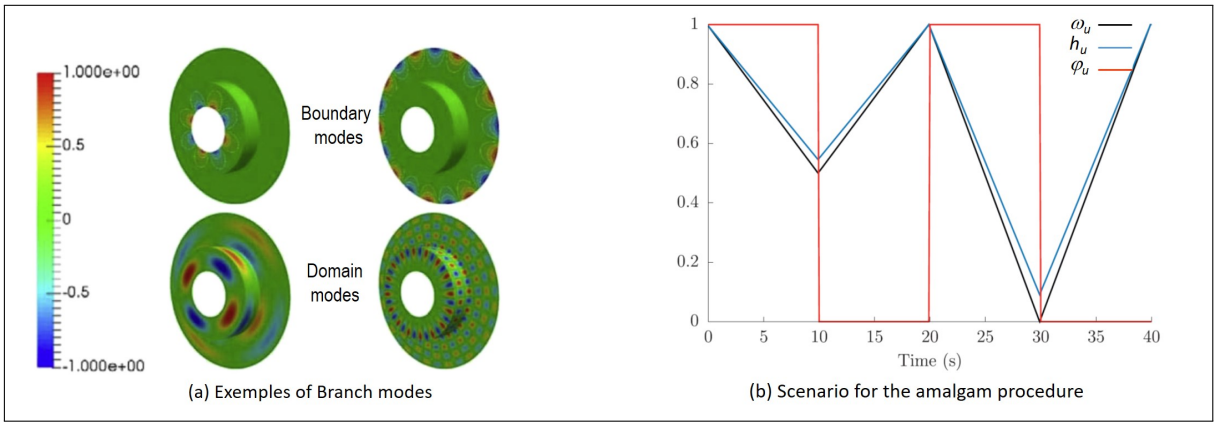

Figure 6: Reduced model

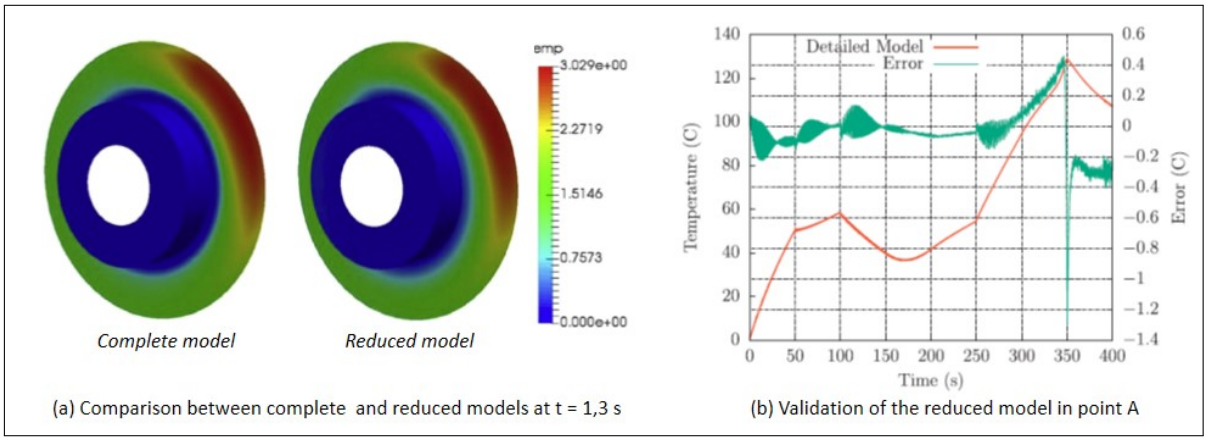

Figure 7: Using the reduced model $\tilde{n} = 15$ in direct simulation

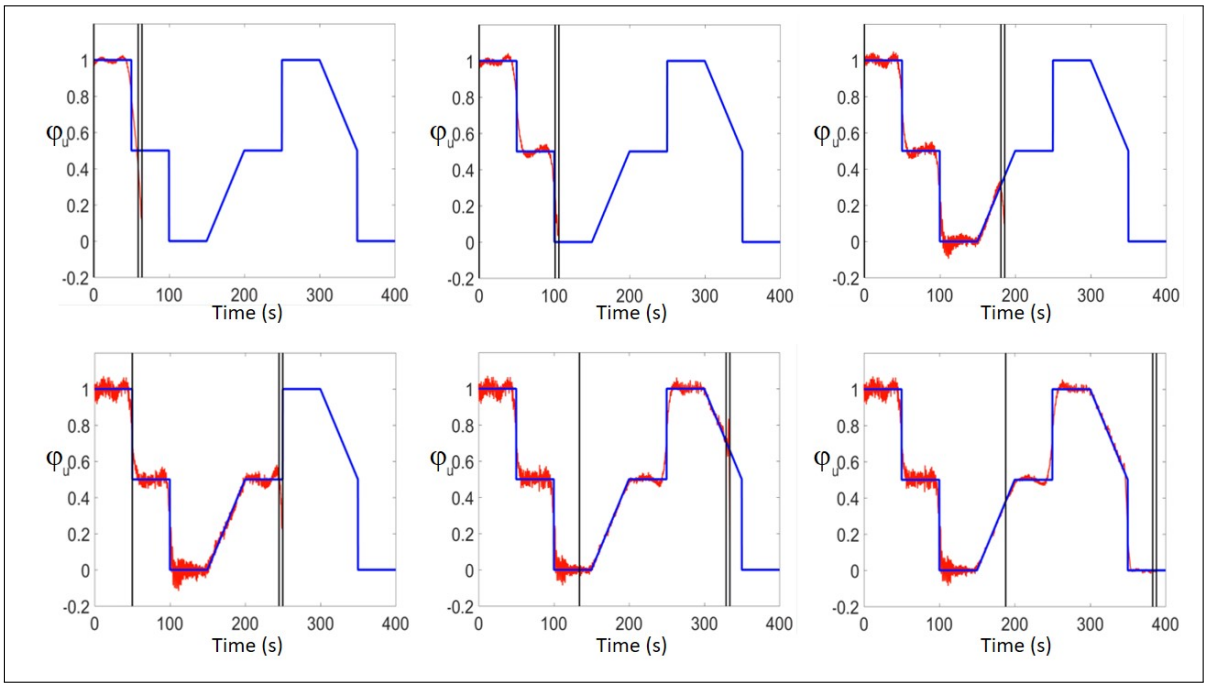

Figure 8: Identification results

6.2 Spatio-temporal identification of heat flux density received by the brake pad [2]

The identification of the spatio-temporal variations of a heat flux density field is addressed in this section. The application relates to the identification of the heat flux received by a brake pad in a braking situation, for which the mechanical deformation and the phenomena of tear and wear cause the appearance of hot spots that one seeks to locate.
We consider a car brake pad for which the complexity of the geometry is respected (Fig. 9.a). It is composed of two materials: the brake lining and its metallic support. This brake pad undergoes three types of boundary conditions (fig 9.b).

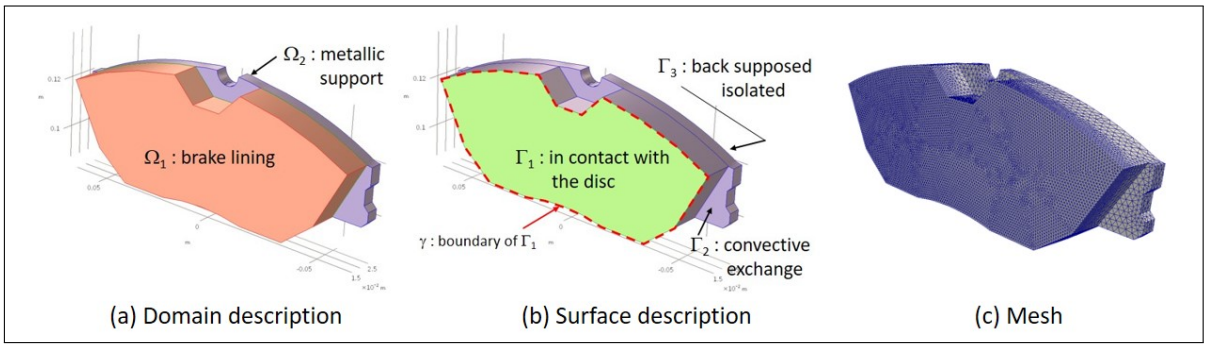

Figure 9: Geometry of the pad and its discretization

6.2.1 Parametrization of the heat flux density

A first Branch base $V^{(\varphi)}$ is used in order to parametrize the heat flux density (fig. 10):

$$\varphi(x,y,t) = \sum_{k=1}^{n^{(\varphi)}} \tilde{x}_k^{(\varphi)}(t)\, \tilde{V}_k^{(\varphi)}(x,y) \tag{62}$$

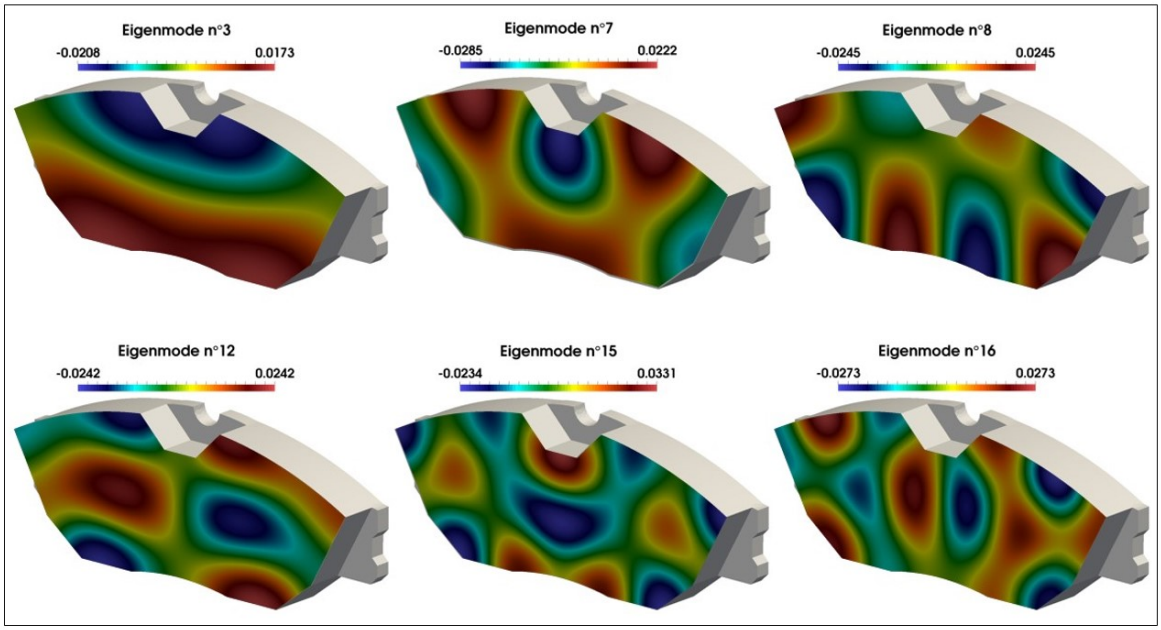

Figure 10: Flux basis

The equation of the heat discretized (eq. 3) becomes then:

$$\mathbf{C}\dot{\mathbf{T}} = (\mathbf{K}+\mathbf{H})\mathbf{T} + \sum_{k=1}^{n^{(\varphi)}} \mathbf{W}\,\tilde{\mathbf{V}}_k^{(\boldsymbol{\varphi})}\,\tilde{x}_k^{(\varphi)} \tag{63}$$

where $\tilde{\mathbf{V}}_k^{(\boldsymbol{\varphi})}$ $[N_{mesh} \times 1]$ is the extension on the domain Ω, of each eigenvector $\tilde{V}_k^{(\varphi)}$ computed on the boundary Γ_1, and where the matrix $\mathbf{W}$ $[N_{mesh} \times N_{mesh}]$ corresponds to the integration of the interpolations functions defined on the border Γ_1 and extended to the domain Ω.
This can be written compactly:

$$\mathbf{C}\dot{\mathbf{T}} = (\mathbf{K}+\mathbf{H})\mathbf{T} + \mathbf{W}\,\tilde{\mathbf{V}}^{(\boldsymbol{\varphi})}\,\tilde{\mathbf{X}}^{(\boldsymbol{\varphi})} \tag{64}$$

where $\tilde{\mathbf{V}}^{(\boldsymbol{\varphi})}$ is a matrix of dimension $[N_{mesh} \times n^{(\varphi)}]$ which gathers all the flux modes $\tilde{\mathbf{V}}_k^{(\boldsymbol{\varphi})}$ $[N_{mesh} \times 1]$ used, and $\tilde{\mathbf{X}}^{(\boldsymbol{\varphi})}$ is the vector of the corresponding states of dimension $[n^{(\varphi)} \times 1]$.

6.2.2 Reduced problem

A second Branch base V^T is used for the temperature field (fig. 11)

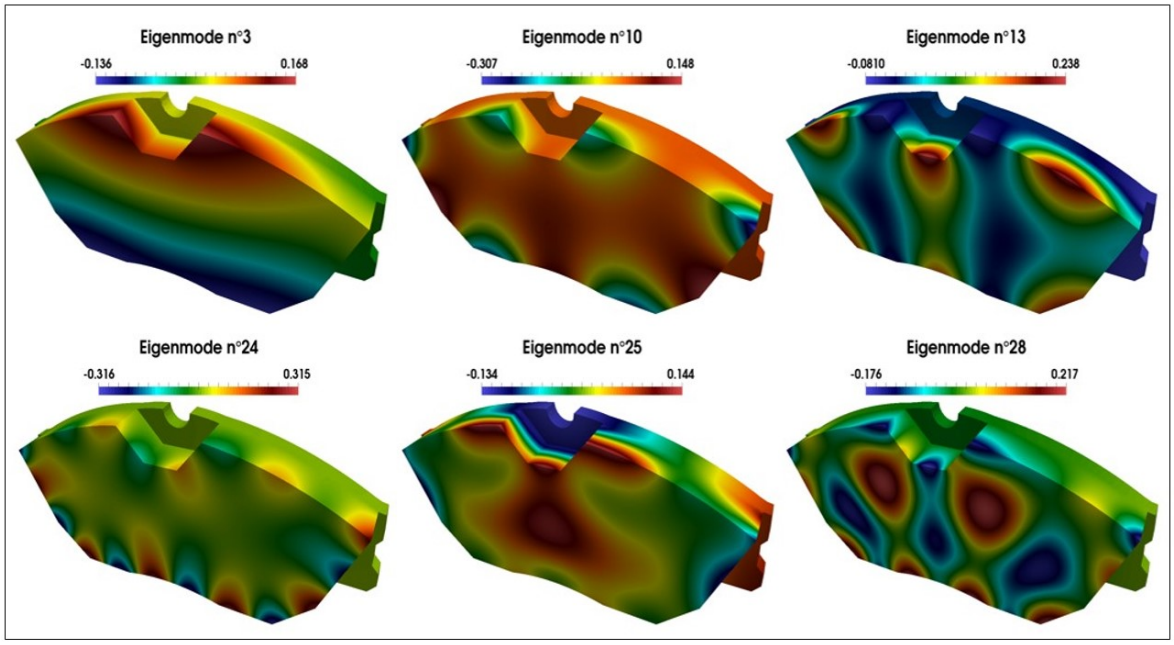

Figure 11: Temperature basis

The reduced modal expression of the thermal problem defined by the equation (10) is then:

$$\mathbf{L}\dot{\tilde{\mathbf{X}}}^{(\mathbf{T})} = \mathbf{M}\,\tilde{\mathbf{X}}^{(\mathbf{T})} + \mathbf{D}\,\tilde{\mathbf{X}}^{(\boldsymbol{\varphi})} \tag{65}$$

with $\mathbf{D} = \tilde{\mathbf{V}}^{(\mathbf{T})t}\ \mathbf{W}\ \tilde{\mathbf{V}}^{(\boldsymbol{\varphi})}$

6.2.3 space time identification

We thus have a temperature model characterized by a few tens of excitation states of temperature x^T (instead of 67353 degrees of freedom of the initial mesh), to identify a few tens of excitation states of flux x^{φ}, instead of the 5945 degrees of freedom of the surface $\Gamma 1$. The

developed technique uses an iterative method of conjugate gradient descent, for which the gradient is estimated by the adjoint method.
The obtained results (Figures 12 and 13) are satisfactory. It can be noted that no specific regularization technique is used in this study (Tikhonov for example). Indeed, in addition to the natural regularization obtained by using a whole time-domain approach and an iterative method, an additional regularization appears, which is induced by the use of the two reduced bases (one for the thermal problem and another for the heat flux parametrization).

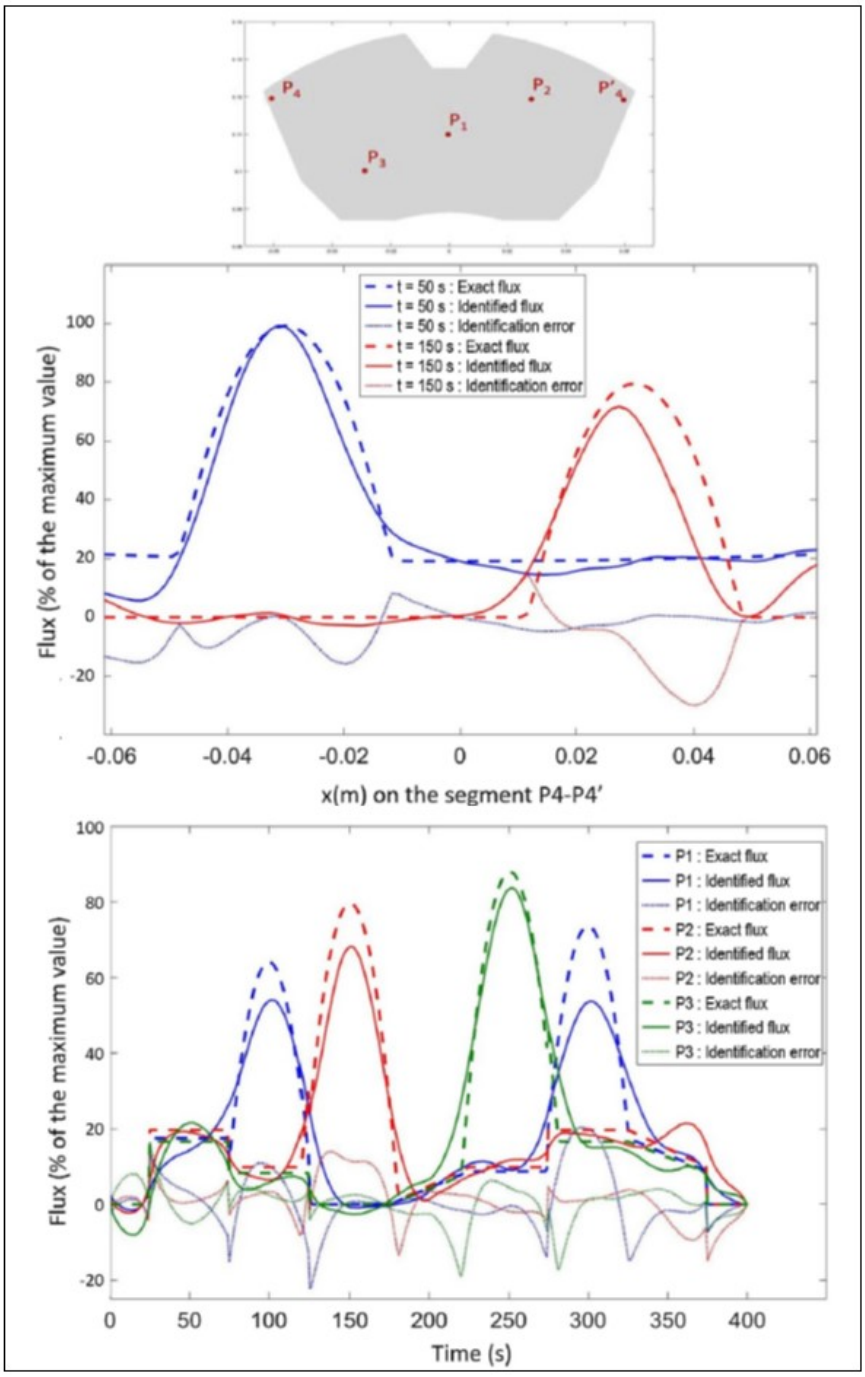

;

Figure 12: Identification results along a segment or versus time

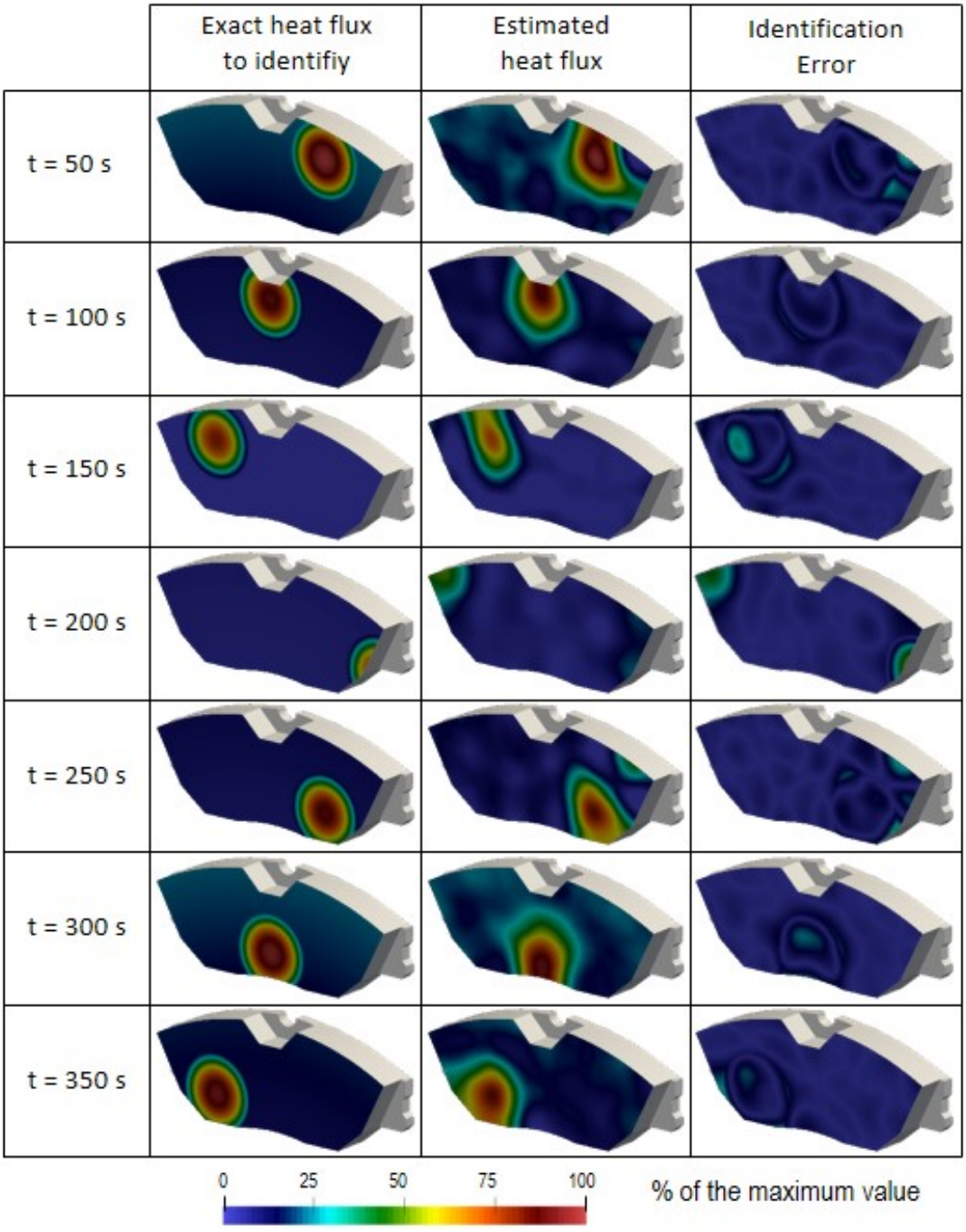

Figure 13: Space-time identification

6.3 On-line indirect thermal measurement in a radiant furnace [3]

6.3.1 The physical problem

Let a heated object on a furnace (Figure 14) in which two radiant tubes dissipate an infra-red radiative heat flux. The power radiated by each tube is driven by the temperature $T_{gas}(t)$ of their intern gas whose value depends on time. The heat exchange between the gas and the tube walls Ω_{tube} is modeled by a global heat exchange coefficient $h_{gas} = 10,000\, W.m^{-2}.K^{-1}$. Given the high temperature level, heat exchange by radiation is preponderant. It is modelled by the radiosity method, which relates the mean flux $\overline{\varphi}_i$ exchanged by patch Ω_i^e to the set of mean temperatures $\overline{T}_j$, with $j \in [1, N_p]$:

$$\forall j \in [1, N_p] \quad \sum_{i=1}^{N_p} \left[\frac{\delta_{ji}}{\varepsilon_i} - \left(\frac{1}{\varepsilon_i} - 1 \right) F_{ji} \right] \overline{\varphi}_i = - \sum_{i=1}^{N_p} \left(\delta_{ji} - F_{ji} \right) \sigma \overline{T}_i^4 \,, \tag{66}$$

where δ_{ji} is the Kronecker delta and F_{ji} are the view factors. This relation (66) can be written in matrix form :

$$\mathbf{A}\, \overline{\varphi} = \mathbf{B}\, \overline{\mathbf{T}}^{\mathbf{4}} \,. \tag{67}$$

The mean flux exchanged by a patch $\overline{\varphi}_j$ expresses as:

$$\overline{\varphi}_j = \sum_{i=1}^{N_p} r_{ji} \overline{T}_i^4 \,, \tag{68}$$

where r_{ji} are the elements of $\mathbf{R}_{rad}\,[N_p,\, N_p] = \mathbf{A}^{-1}\,\mathbf{B}$.

This radian flux is included in the heat equation defined on the solid domains of the scene (wall, tubes, stand, etc) , whicb can be written after s(Figure 14) :

$$\mathbf{C} \frac{d\mathbf{T}}{dt} = [\mathbf{K} + \mathbf{H}]\, \mathbf{T} + \mathbf{U_{cpl}}\, T_{int}\,(\mathbf{T}) + \mathbf{U_0} + \overline{\mathbf{R}}_{rad} \overline{\mathbf{T}}^4 + T_{gas}(t)\ \mathbf{U_{tube}} \,. \tag{69}$$

In this equation:

- Vector $\mathbf{T}$ contains the temperature value at the N discretization points.
- $\mathbf{C}$, $\mathbf{K}$ and $\mathbf{H}$ are $[N \times N]$ symmetric sparse matrices: $\mathbf{C}$ is the thermal inertia matrix, $\mathbf{K}$ the conductivity matrix and $\mathbf{H}$ gathers the different convection terms on Ω_{ext}, Ω_{int} and Ω_{tube}.
- Vector $\mathbf{U_0}$ corresponds to the external known solicitations and $\mathbf{U_{cpl}}$ represents the convective exchange with the air inside the furnace, at temperature that depends on the temperature of all internal surfaces $T_{int}\,(\mathbf{T})$:

$$T_{int}\,(T) = \frac{\int\limits_{\Omega_{int}} h_{int}\ T\ d\Omega}{\int\limits_{\Omega_{int}} h_{int}\ d\Omega} \,. \tag{70}$$

  We obtein after discretization :

$$T_{int}\,(\mathbf{T}) = \mathbf{D}\,\mathbf{T} \,. \tag{71}$$

- Vector $\overline{\mathbf{T}}^4$ of dimension $[N_p]$ contains mean temperatures of every patch Ω_i^e. Radiation matrix $\overline{\mathbf{R}}_{rad}$ $[N \times N_p]$ allots the mean heat flux density from the N_p patches to the N nodes.

$$\overline{\mathbf{T}} = \mathbf{U_R}\,\mathbf{T}\,, \tag{72}$$

- Finally, vector $\mathbf{U_{tube}}$ of dimension $[N]$ stands for the heat source generated by the gas combustion inside the radiant tubes.

6.3.2 Identification and reconstruction of the thermal field

The goal is to recover the whole thermal field of the heated object from a few measurement points (A, B and C on figure 14). The radiant thermal source is first identified via a low order reduced model based on AROMM method (Figure 15).

From this identified temperature, the thermal field is then recovered by direct simulation using a reduced model of higher order which leads to a better precision.

The whole identification procedure lasts less than $5\,000\,s$, which is ten times smaller the duration of the thermal process ($50\,000\,s$). The whole thermal field of the heated object is refreshed every $200\,s$ with an average precision of $\bar{\sigma} = 2.9\,K$, which is below the measurement noise.

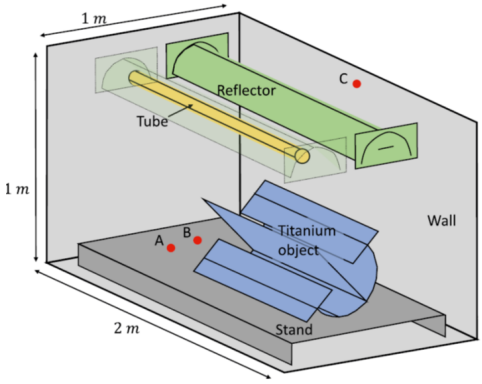

Figure 14: The considered geometry

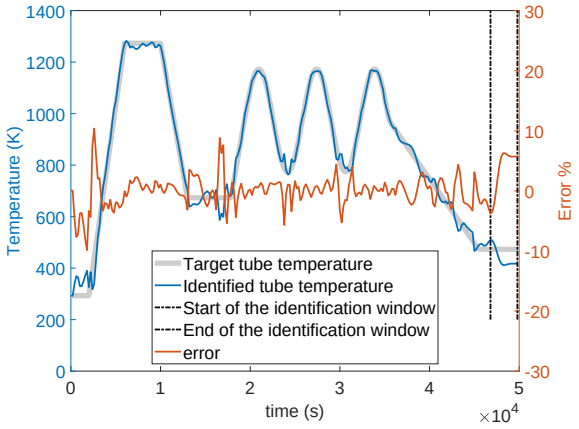

Figure 15: Identification results with $\widetilde{N}_{(rec)} = 20$ modes and $\sigma_N = 5\,K$.

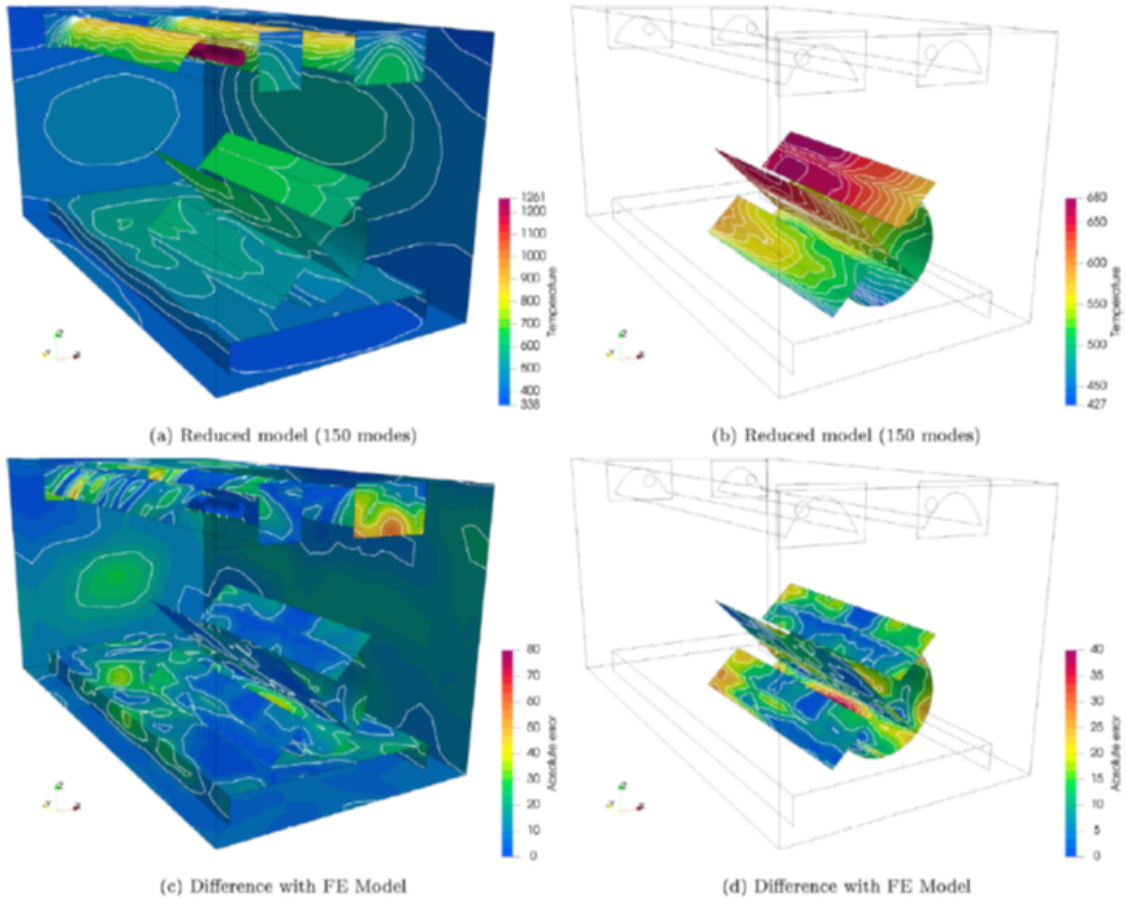

Figure 16: Temperature and error fields at $t = 6\,000\,s$ for reconstruction with $\widetilde{N}_{(rec)} = 150$ modes in the case of identification with $\widetilde{N}_{(id)} = 20$ modes and $\sigma_N = 5\,K$.

References

[1] S. Carmona, Y. Rouizi, O. QuÃ©mÃ©ner, F. Joly, A. Neveu, Estimation of heat flux by using reduced model and the adjoint method. application to a brake disc rotating (2018).

[2] S. Carmona, Y. Rouizi, O. QuÃ©mÃ©ner, Spatio-temporal identification of heat flux density using reduced models. application to a brake pad, International journal of heat and mass transfer 128 (2019) 1048–1063.

[3] B. Gaume, F. Joly, O. Quéméner, Modal reduction for a problem of heat transfer with radiation in an enclosure, International Journal of Heat and Mass Transfer-doi:https://doi.org/10.1016/j.ijheatmasstransfer.2019.07.039.

[4] S. Grosjean, F. Joly, K. Vera, A. nevau, E. Monier-Vinard, Reduction of an electronic card thermal problem by the modal substructuring method, 16th International Hreat Transfer Conference, August 10-15, Beijing, China.

[5] A. Fic, R. Bialecki, A. Kassab, Solving transient nonlinear heat conduction problems by proper orthogonal decomposition and the finite-element method, Numerical Heat Transfer, Part B: Fundamentals 48 (2) (2005) 103–124. arXiv:http://dx.doi.org/10.1080/10407790590935920, doi:10.1080/10407790590935920.

[6] X. Zhang, H. Xiang, A fast meshless method based on proper orthogonal decomposition for the transient heat conduction problems, International Journal of Heat and Mass Transfer 84 (2015) 729 – 739. doi:http://dx.doi.org/10.1016/j.ijheatmasstransfer.2015.01.008.

[7] R. Ghosh, Y. Joshi, Error estimation in pod-based dynamic reduced-order thermal modeling of data centers, International Journal of Heat and Mass Transfer 57 (2) (2013) 698 – 707. doi:http://dx.doi.org/10.1016/j.ijheatmasstransfer.2012.10.013.

[8] A. Sempey, C. Inard, C. Ghiaus, C. Allery, Fast simulation of temperature distribution in air conditioned rooms by using proper orthogonal decomposition, Building and Environment 44 (2) (2009) 280 – 289. doi:http://dx.doi.org/10.1016/j.buildenv.2008.03.004.

[9] J. García, J. Cabeza, A. Rodríguez, Two-dimensional non-linear inverse heat conduction problem based on the singular value decomposition, International Journal of Thermal Sciences 48 (6) (2009) 1081 – 1093. doi:http://dx.doi.org/10.1016/j.ijthermalsci.2008.09.002.

[10] A. Rajabpour, F. Kowsary, V. Esfahanian, Reduction of the computational time and noise filtration in the IHCP by using the proper orthogonal decomposition POD method, International Communications in Heat and Mass Transfer 35 (8) (2008) 1024 – 1031. doi:http://dx.doi.org/10.1016/j.icheatmasstransfer.2008.05.004.

[11] H. Park, M. Sung, Sequential solution of a three-dimensional inverse radiation problem, Computer Methods in Applied Mechanics and Engineering 192 (33) (2003) 3689 – 3704. doi:http://dx.doi.org/10.1016/S0045-7825(03)00370-0.

[12] W. Adamczyk, Z. Ostrowski, Retrieving thermal conductivity of the solid sample using reduced order model inverse approach, International Journal of Numerical Methods for Heat & Fluid Flow 27 (3) (2017) 729–739. arXiv:https://doi.org/10.1108/HFF-05-2016-0206, doi:10.1108/HFF-05-2016-0206.

[13] M. Girault, D. Petit., Identification methods in nonlinear heat conduction. Part I: Model Reduction, International Journal of Heat and Mass Transfer 48 (2005) 105–118.

[14] M. Girault, D. Petit, Identification methods in nonlinear heat conduction. Part II: inverse problem using a reduced model, International Journal of Heat and Mass Transfer 48 (1) (2005) 119 – 133. doi:DOI: 10.1016/j.ijheatmasstransfer.2004.06.033.

[15] E. Videcoq, M. Girault, V. Ayel, C. Romestant, Y. Bertin, On-line thermal regulation of a capillary pumped loop via state feedback control using a low order model, Applied Thermal Engineering 108 (2016) 614 – 627. doi:http://dx.doi.org/10.1016/j.applthermaleng.2016.07.071.

[16] M. Girault, E. Videcoq, D. Petit, Estimation of time-varying heat sources through inversion of a low order model built with the modal identification method from in-situ temperature measurements, International Journal of Heat and Mass Transfer 53 (1) (2010) 206 – 219. doi:http://dx.doi.org/10.1016/j.ijheatmasstransfer.2009.09.040.

[17] K. Bouderbala, H. Nouira, E. Videcoq, M. Girault, D. Petit, MIM, FEM and experimental investigations of the thermal drift in an ultra-high precision set-up for dimensional metrology at the nanometre accuracy level, Applied Thermal Engineering 94 (2016) 491 – 504. doi:http://dx.doi.org/10.1016/j.applthermaleng.2015.09.092.

[18] E. Videcoq, M. Girault, A. Piteau, Thermal control via state feedback using a low order model built from experimental data by the modal identification method,

International Journal of Heat and Mass Transfer 55 (5) (2012) 1679 – 1694. doi:http://dx.doi.org/10.1016/j.ijheatmasstransfer.2011.11.023.

[19] J. Berger, S. Guernouti, M. Woloszyn, F. Chinesta, Proper generalised decomposition for heat and moisture multizone modelling, Energy and Buildings 105 (2015) 334 – 351. doi:http://dx.doi.org/10.1016/j.enbuild.2015.07.021.

[20] J. Berger, W. Mazuroski, N. Mendes, S. Guernouti, M. Woloszyn, 2d whole-building hygrothermal simulation analysis based on a pgd reduced order model, Energy and Buildings 112 (2016) 49 – 61. doi:http://dx.doi.org/10.1016/j.enbuild.2015.11.023.

[21] J. Berger, N. Mendes, An innovative method for the design of high energy performance building envelopes, Applied Energy 190 (2017) 266 – 277. doi:http://dx.doi.org/10.1016/j.apenergy.2016.12.119.

[22] D. González, F. Masson, F. Poulhaon, A. Leygue, E. Cueto, F. Chinesta, Proper generalized decomposition based dynamic data driven inverse identification, Mathematics and Computers in Simulation 82 (9) (2012) 1677 – 1695. doi:http://dx.doi.org/10.1016/j.matcom.2012.04.001.

[23] C. Lanczos, An iteration method for the solution of the eigenvalue problem of linear differential and integral operators, Journal of Research of the National Bureau of Standards 45 (1950) 255–282. doi:10.6028/jres.045.026.

[24] R. Radke, A matlab implementation of the implicitly restarted arnoldi method for solving large-scale eigenvalues problems, Ph.D. thesis, A thesis submitted in partial fullfillment of the requirements for the degree Master of Arts, Rice University, Houston, Texas (1996).

[25] R. Lehoucq, D. Sorensen, C. Yang, ARPACK Users' Guide: Solution of Large-scale Eigenvalue Problems with Implicitly Restarted Arnoldi Methods, SIAM e-books, Society for Industrial and Applied Mathematics (SIAM, 3600 Market Street, Floor 6, Philadelphia, PA 19104), 1998.

[26] J. Sicard, P. Bacot, A. Neveu, Analyse modale des échanges thermiques dans le bâtiment, International Journal of Heat and Mass Transfer 28 (1) (1985) 111 – 123. doi:http://dx.doi.org/10.1016/0017-9310(85)90013-4.

[27] P. Bacot, A. Neveu, J. Sicard, Analyse modale des phénomènes thermiques en régime variable dans le bâtiment, Revue Générale de Thermique 267 (1984) 189–201.

[28] G. Lefebvre, J. Bransier, A. Neveu, Simulation du comportement thermique d'un local par des méthodes numériques d'ordre réduit, Revue Générale de Thermique 302 (1987) 106–114.

[29] J. Salgon, A. Neveu, Application of modal analysis to modelling of thermal bridges in buildings, Energy and Buildings 10 (2) (1987) 109 – 120. doi:http://dx.doi.org/10.1016/0378-7788(87)90013-2.

[30] A. Neveu, K. El-Khoury, B. Flament, Simulation de la conduction non linéaire en régime variable: décomposition sur les modes de branche, International Journal of Thermal Sciences 38 (4) (1999) 289 – 304. doi:http://dx.doi.org/10.1016/S1290-0729(99)80095-7.

[31] O. Quéméner, A. Neveu, E. Videcoq, A specific reduction method for the branch modal formulation: Application to a highly non-linear configuration, International Journal of Thermal Sciences 46 (9) (2007) 890 – 907. doi:DOI: 10.1016/j.ijthermalsci.2006.11.011.

[32] E. Videcoq, O. Quéméner, W. Nehme, A. Neveu, Real time heat sources identification by a branch eigenmodes reduced model, in: 6th International Conference on Inverse Problems in Engineering, Theory and Practice, Dourdan (France), and in Journal of Physics: Conference Series 135 (freely available on line, paper n 012101), 2008.

[33] E. Videcoq, O. Quéméner, M. Lazard, A. Neveu, Heat source identification and on-line temperature control by a branch eigenmodes reduced model, International Journal of Heat and Mass Transfer 51 (19-20) (2008) 4743 – 4752. doi:DOI: 10.1016/j.ijheatmasstransfer.2008.02.029.

[34] E. Videcoq, M. Lazard, O. Quéméner, A. Neveu, Online temperature prediction using a branch eigenmode reduced model applied to cutting process, Numerical Heat Transfer, Part A: Applications 55 (7) (2009) 683–705. arXiv:http://dx.doi.org/10.1080/10407780902821490, doi:10.1080/10407780902821490.

[35] F. Joly, O. Quéméner, A. Neveu, Modal reduction of an advection-diffusion model using a branch basis, Numerical Heat Transfer, Part B: Fundamentals 53 (5) (2008) 466–485. doi:10.1080/10407790701849550.

[36] O. Quéméner, F. Joly, A. Neveu, On-line heat flux identification from a rotating disk at variable speed, International Journal of Heat and Mass Transfer 53 (7) (2010) 1529 – 1541. doi:http://dx.doi.org/10.1016/j.ijheatmasstransfer.2009.11.032.

[37] P. Laffay, O. Quéméner, A. Neveu, Developing a method for coupling branch modal models, International Journal of Thermal Sciences 48 (6) (2009) 1060 – 1067. doi:http://dx.doi.org/10.1016/j.ijthermalsci.2008.11.002.

[38] P. O. Laffay, O. Quéméner, A. Neveu, B. Elhajjar, The modal substructuring method: An efficient technique for large-size numerical simulations, Numerical Heat Transfer, Part B: Fundamentals 60 (4) (2011) 278–304. doi:10.1080/10407790.2011.609113.

[39] S. Marshall, An approximation method for reducing the order of linear system, control (1966) 642–643.

[40] O. Quéméner, J. Battaglia, A. Neveu, Résolution d'un problème inverse par utilisation d'un modèle réduit modal. application au frottement d'un pion sur un disque en rotation, International Journal of Thermal Sciences 42 (4) (2003) 361 – 378. doi:http://dx.doi.org/10.1016/S1290-0729(02)00037-6.

[41] A. Oulefki, Réduction des modèles thermiques par amalgame modal, Ph.D. thesis, Ecole Nationale de Ponts et Chaussées (1993).

[42] G. Benjamin, Réduction d'un problème d'auto-rayonnement par modes de branche : application aux échanges thermiques dans un domaine multi-enceintes, Ph.D. thesis, Paris Saclay (2016).

[43] N. Brou, Modélisation et commande d'un système de cogénération utilisant des énergies renouvelables pour le bâtiment, Ph.D. thesis, Paris Saclay (2015).

[44] O. Quéméner, F. Joly, A. Neveu, The generalized amalgam method for modal reduction, International Journal of Heat and Mass Transfer 55 (4) (2012) 1197 – 1207. doi:http://dx.doi.org/10.1016/j.ijheatmasstransfer.2011.09.043.